MCB
Journals.ASM.org

Rac1 Activation in Podocytes Induces Rapid Foot Process Effacement and Proteinuria

Haiyang Yu,[a] Hani Suleiman,[a] Alfred H. J. Kim,[b] Jeffrey H. Miner,[c] Adish Dani,[a] Andrey S. Shaw,[a,d] Shreeram Akilesh[a]*

Department of Pathology and Immunology,[a] Division of Rheumatology[b] and Renal Division,[c] Department of Internal Medicine, and Howard Hughes Medical Institute,[d] Washington University School of Medicine, St. Louis, Missouri, USA

The kidney's vital filtration function depends on the structural integrity of the glomerulus, the proximal portion of the nephron. Within the glomerulus, the architecturally complex podocyte forms the final cellular barrier to filtration. Injury to the podocyte results in a morphological change called foot process effacement, which is a ubiquitous feature of proteinuric diseases. The exact mechanism underlying foot process effacement is not known, but recently it has been proposed that this change might reflect activation of the Rac1 GTPase. To test this hypothesis, we generated a podocyte-specific, inducible transgenic mouse line that expressed constitutively active Rac1. When the Rac1 transgene was induced, we observed a rapid onset of proteinuria with focal foot process effacement. Using superresolution imaging, we verified that the induced transgene was expressed in damaged podocytes with altered foot process morphology. This work sheds new light on the complex balance of Rho GTPase signaling that is required for proper regulation of the podocyte cytoskeleton.

The structural integrity of the proximal portion of the nephron, the glomerulus, is vital to the kidney's filtration function. Within the glomerular capillary tuft, the kidney's filtration barrier is a biomechanical composite of fenestrated endothelial cells, a thick glomerular basement membrane, and complex visceral epithelial cells called podocytes. Podocytes lie on the outer aspect of glomerular capillaries and extend cytoplasmic processes (foot processes) that interdigitate with those from neighboring podocytes to form a mesh-like network that constitutes the final barrier to filtration. These podocyte foot processes consist of a network of highly organized actin cytoskeleton structures. Under conditions of podocyte injury, these foot processes are flattened and simplified ("effaced"). This change in the podocyte's cytoskeleton is often seen in patients with diseases characterized by spillage of serum proteins into the urine (proteinuria). Defects in actin-regulatory proteins lead to irreversible podocyte injury and focal and segmental glomerulosclerosis (FSGS), a disease that is typified by proteinuria, in humans and in animal models (1, 2).

Numerous cell culture systems point to a critical role for Rho-family GTPases in actin cytoskeleton remodeling, with RhoA activation inducing actin bundling and Rac1 activation inducing lamellipodia (3). After receiving diverse signaling inputs, members of the Rho family of small GTPases act through their effectors to polymerize and organize actin filaments into various configurations that deform the cell membrane and change the cell shape. During podocyte foot process effacement, the bundled actin cytoskeleton of the foot processes is reorganized into broad membrane sheets that resemble the lamellipodia seen in cultured cells. As in *in vitro* studies, small GTPases of the Rho family (exemplified by RhoA, Cdc42, and Rac1) and their regulators have been implicated in dynamic shape changes seen in podocytes both during development and in disease states (4). Of the three major Rho-family GTPases, Cdc42 has been shown to be critical for podocyte development, while both RhoA and Rac1 seem dispensable in early stages (5). After this initial phase, RhoA and Rac1 seem to play more-important roles in podocyte biology. In many biological systems, including podocytes, RhoA and Rac1 antagonize each other's activation and function (6, 7).

Some groups have proposed that preferential activation of RhoA is pathogenic to podocytes and can cause podocyte foot process effacement and proteinuria (8, 9). This is surprising given that (i) the proteinuria in this model system took weeks to develop, while activation of Rho-family GTPases *in vitro* causes rapid cytoskeletal rearrangement (10, 11), and (ii) the introduction of dominant negative (DN) RhoA produces a phenotype similar to that of a constitutively active RhoA transgene (9).

Therefore, we and others have proposed that excessive Rac1 (and/or Cdc42) activation or inhibition of Rho activity might be the key step in podocyte injury. Although podocyte-specific loss of Rac1 has no effect during podocyte development, loss of Rac1 protects against foot process effacement induced by protamine sulfate infusion (2). Synaptopodin, a podocyte actin-binding protein, reinforces RhoA signaling and suppresses Cdc42 signaling to promote proper cytoskeletal architecture (12, 13). Genetic ablation of synaptopodin in mice results in increased susceptibility to proteinuria (14, 15). Deletion of Rho GDP dissociation inhibitor alpha (RhoGDIα) (a negative regulator of Rho-family GTPases) in mice results in foot process effacement and proteinuria that correlates with increased Rac1 activity (16). Patients with mutations in ARHGDIA also demonstrate increased Rac1 and Cdc42 activity, podocyte foot process effacement, and proteinuria (17, 18). Mutations in the GTPase-activating protein Arhgap24 result

Received 12 June 2013 **Returned for modification** 10 July 2013
Accepted 18 September 2013
Published ahead of print 23 September 2013
Address correspondence to Andrey S. Shaw, ashaw@wustl.edu.
* Present address: Shreeram Akilesh, Department of Pathology, University of Washington, Seattle, Washington, USA.
Supplemental material for this article may be found at http://dx.doi.org/10.1128/MCB.00730-13.

doi:10.1128/MCB.00730-13

in increased Rac1 activation *in vitro* and are correlated with podocyte injury and FSGS in patients (19).

These studies suggest that inappropriate Rac1 activation plays a pathogenic role in podocyte foot process effacement and proteinuria. However, the effects of Rac1 activation in podocytes have been studied only indirectly, through the manipulation of upstream regulatory proteins (16–19). Therefore, to test directly whether Rac activation induces podocyte foot process effacement, we generated a double transgenic system in mice in which green fluorescent protein (GFP)-tagged constitutively active Rac1 (Rac1Q61L) was expressed in podocytes after induction with doxycycline (DOX). We observed rapid onset of proteinuria within 2 days of DOX induction. The degree of proteinuria correlated with the level of active Rac1 expression. However, proteinuria in this system was not durable; it decreased gradually over the course of a month despite continuous exposure to DOX. Thus, activation of Rac1 in podocytes rapidly causes foot process effacement and proteinuria *in vivo*. These results are distinct from the effects of RhoA activation in podocytes and emphasize the complex interplay of small GTPase signaling in the regulation of podocyte shape and function.

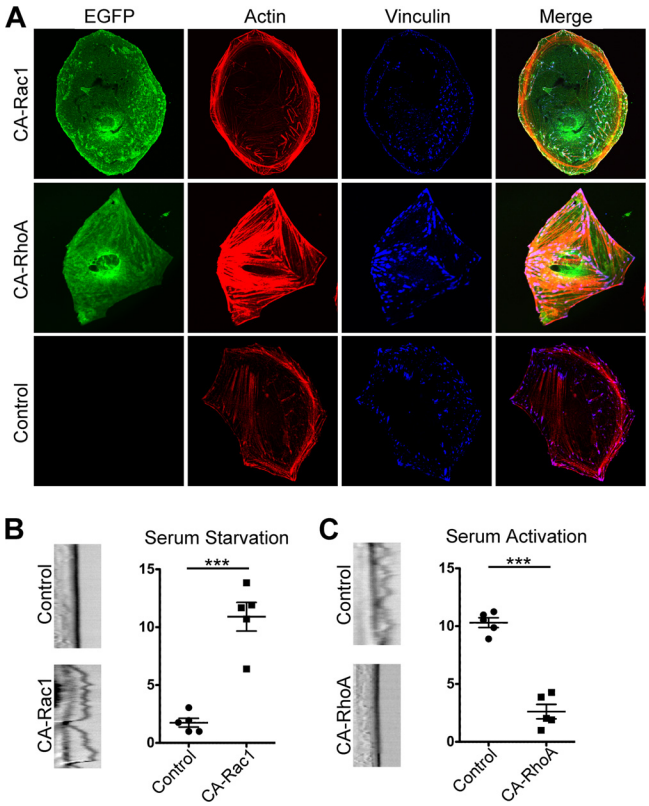

FIG 1 Constitutively active Rho-family GTPases exert opposing effects on the actin cytoskeletons of podocytes. (A) Immunofluorescence imaging was performed on differentiated mouse podocytes that were stably transduced with EGFP_CA-Rac1 or EGFP_CA-RhoA (green). The filamentous actin network was delineated with phalloidin (red), and focal adhesions and contacts were identified with vinculin (blue). Compared to the morphology of control, untransduced cells, EGFP_CA-Rac1 induced flattening of the cell and lamellipodium formation, while EGFP_CA-RhoA induced numerous stress fibers and cell contraction. (B) Under conditions of serum starvation, podocytes exhibited minimal membrane ruffling activity, as determined by kymographic analysis. The introduction of EGFP_CA-Rac1 significantly increased membrane dynamics and ruffling. The *y* axes in panels B and C show actin spike length (in arbitrary units). Asterisks indicate a significant difference ($P < 0.0001$) by the unpaired *t* test. (C) Exposure of starved cells to serum also induced membrane ruffling, which was suppressed by the introduction of EGFP_CA-RhoA.

MATERIALS AND METHODS

Generation of EGFP_CA-Rac1 knock-in transgenic mice. We chose the *Hprt1* locus (on mouse chromosome X) for targeting because it is a nonessential housekeeping gene that encodes a selectable marker (20, 21). The pHPRT targeting vector was generated on a pBluescript SKII(−) backbone by PCR amplifying the left arm (a 5.1-kb fragment upstream of exon 1) and right arm (a 2.1-kb fragment downstream of exon 1) of the *Hprt1* gene from a bacterial artificial chromosome (RP24-335G16). The tetracycline-responsive promoter element (TRE), enhanced GFP (EGFP), Rac1Q61L, and bovine growth hormone polyadenylation signal (bGH-polyA) sequences were amplified by PCR and were inserted sequentially into the pHPRT targeting vector. The KH2 embryonic stem (ES) cell line harboring the *Rosa26*-reverse tetracycline transactivator (rtTA) transgene (on mouse chromosome 6) was used for transfection. Cells with homologous recombination of the transgene into the *Hprt1* locus were selected on the basis of their growth in the presence of 6-thioguanine, which is toxic to cells expressing functional *Hprt1*. Appropriate single-copy insertion of the EGFP_CA-Rac1 transgene into the *Hprt1* locus was confirmed by PCR. Targeted ES cells were injected into blastocysts to generate chimeric mice. Because they are on separate chromosomes, the *Rosa26*-rtTA and EGFP_CA-Rac1 transgenes segregated in subsequent breedings. The EGFP_CA-Rac1 single transgenic line was maintained on a C57BL/6J × 129/SvJ mixed genetic background. EGFP genotyping primers (a protocol from The Jackson Laboratory) were used for genotyping (Forward_oIMR0872, 5′-AAGTTCATCTGCACCACCG-3′; Reverse_oIMR1416, 5′-TCCTTGAAGAAGATGGTGCG-3′); internal positive-control primers were Forward_oIMR7338 (5′-CTAGGCCACAGAATTGAAAGATCT-3′) and Reverse_oIMR7339 (5′-GTAGGTGGAAATTCTAGCATCATCC-3′). All animal experiments were conducted with the approval of the Washington University Animal Studies Committee.

Mouse strains and transgene induction. The NPHS2-rtTA (POD-rtTA) strain was obtained from Jeffrey Kopp at the NIH (22). The *Nphs1*-rtTA-3G (NEF-rtTA) strain will be described in detail elsewhere (34). All mice used in this study were male, and therefore, each carried only one copy of the EGFP_CA-Rac1 transgene on his single X chromosome. To induce transgene expression, regular chow was replaced with DOX-supplemented chow (2,000 ppm; TestDiet) for the times indicated in the figures.

Cell culture and cell-based assays. Immortalized murine podocytes were maintained and differentiated as described previously (19). For live-cell imaging assays, podocytes were infected with lentiviral vectors encoding N-terminally EGFP tagged CA-Rac1 and CA-RhoA. An empty EGFP vector was used as a control.

Antibodies. Antibodies for immunostaining included rabbit anti-podocin (P0372; dilution, 1:400; Sigma-Aldrich), goat antinephrin (AF3159; dilution, 1:100; R&D Systems), rabbit anti-laminin β2 (23) (dilution, 1:1,500), rabbit anti-WT1 (SC-192; dilution, 1:200; Santa Cruz), and chicken anti-GFP (A10262; dilution, 1:500; Invitrogen). The antibodies used for immunoblotting were mouse anti-XFP (632381; dilution, 1:10,000; Clontech), rabbit anti-ERK2 (sc-154; dilution, 1:5,000; Santa Cruz Biotechnology), and rabbit antipodocin (P0372; dilution, 1:500; Sigma-Aldrich). Fluorescently conjugated secondary antibodies were purchased from Jackson ImmunoResearch, and stochastic optical reconstruction microscopy (STORM) antibodies were conjugated as described previously (24).

Immunofluorescence assays. Fresh kidney tissue was embedded in OCT compound and was snap-frozen on dry ice. Cryosections (8 μm) were applied to charged slides. Cultured podocytes were seeded onto collagen I-coated coverslips. For immunofluorescence assays, the tissue sections or coverslips containing podocytes were fixed with 1% paraformal-

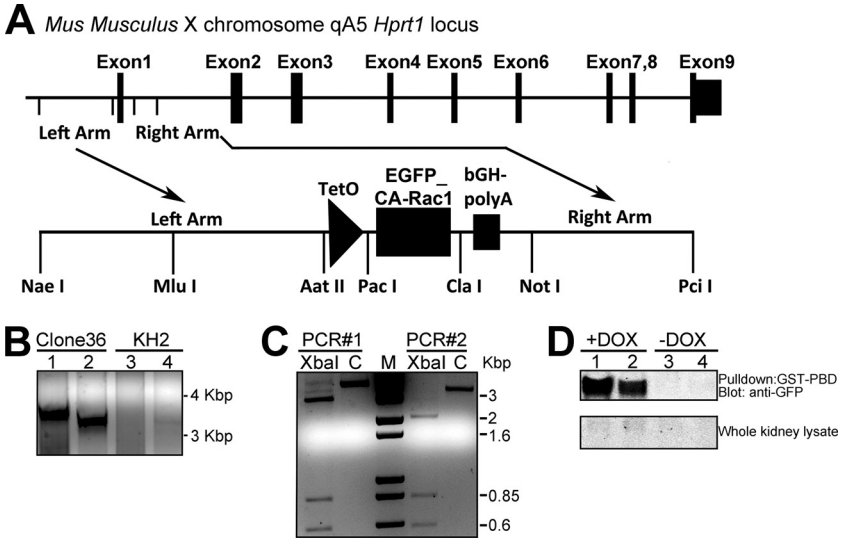

FIG 2 Generation of inducible EGFP_CA-Rac1 transgenic mice. (A) Strategy for targeted insertion of inducible EGFP_CA-Rac1 into exon 1 of the murine *Hprt1* locus on chromosome X. The tetracycline response element (TRE) allows DOX-inducible EGFP_CA-Rac1 expression when this mouse line is crossed to lineage-specific rtTA-transgenic mouse lines. (B) Confirmation of targeted insertion and verification of EGFP_CA-Rac1 activity in transgenic mice. Long genomic PCR for the 5′ and 3′ insertion sites confirmed homologous recombination in ES cell clone 36. Parental KH2 ES cells were used as the negative control. Lanes 1 and 3, PCR with Primer1 (in the 5′ EGFP transgene sequence) and Primer3 (400 bp downstream of the 3′ arm); lanes 2 and 4, genomic PCR with Primer2 (in the Rac1 transgene sequence) and Primer3. (C) XbaI digestion produced specific digestion bands (400 bp and 600 bp) that confirmed the specificity of the 5′ and 3′ targeted locus PCR products from panel B. Results for two replicates are shown. Lanes C, control PCR product without XbaI digestion. (D) Transgenically expressed EGFP_CA-Rac1 is functionally active. EGFP_CA-Rac1 transgenic mice were crossed to POD-rtTA inducer mice to generate POD×Rac1 mice. The EGFP_CA-Rac1 transgene was induced by feeding DOX to the mice. Transgenically expressed EGFP_CA-Rac1 binds to GST-PBD, which specifically recognizes the active conformation of Rac1. Transgenic EGFP_CA-Rac1 (detected with an anti GFP antibody) is not induced, and is not present to bind to GST-PBD, without DOX induction. Representative data from two induced and noninduced POD×Rac1 mice are shown.

dehyde (PFA) in phosphate-buffered saline (PBS) for 5 min, followed by blocking and permeabilization with 2% fetal bovine serum (FBS) in PBS with 0.1% saponin. Primary antibodies at the dilutions given above were applied for 1 h at room temperature. After extensive washes with PBS, fluorescently conjugated secondary antibodies were applied at a 1:500 dilution for another hour at room temperature. After washing, the prepared slides were imaged on an Olympus FV1000 spinning-disc confocal microscope.

Albumin-creatinine assay. Mouse urine samples were collected at the time points indicated in the figures, and urinary albumin (E90-134; Bethyl) and creatinine (DICT-500; BioAssay Systems) were quantified by enzyme-linked immunosorbent assays (ELISA) according to the manufacturers' protocols.

Transmission electron microscopy (TEM). Portions of kidney cortex were fixed with 2% paraformaldehyde and 2% glutaraldehyde. Specimen processing, ultrathin sectioning, and imaging were performed by the Electron Microscopy (EM) Core Facility at Washington University.

STORM imaging and EM-STORM correlation. The method developed to perform STORM-EM correlation has been described recently (25). Kidney tissue was labeled with a rabbit anti-laminin β2 antibody and an anti-GFP antibody. Donkey anti-mouse and donkey anti-rabbit secondary antibodies (Jackson ImmunoResearch) were custom conjugated to the Alexa 647 reporter dye and either the Alexa 405 or the Cy3 activator dye as described previously (24). Images were acquired using a custom-made setup as described previously (26). Approximately 10,000 images per channel were captured and were analyzed using custom software. After STORM imaging, the tissue sections were fixed in 2% glutaraldehyde and were prepared for electron microscopy. Areas of the cover glass that were imaged for STORM were cut, rinsed in distilled water (dH_2O), deep-frozen, etched, and replicated with ~2-nm platinum deposition. After the glass was dissolved in concentrated hydrofluoric acid, replicas were rinsed in distilled water, transferred to Luxel grids (Luxel, Friday Harbor, WA), and photographed on a JEOL 1400 microscope with an Advanced Microscopy Techniques (AMT) digital camera attached. The EM images were matched with the corresponding STORM images and were superimposed using Adobe Photoshop. Image manipulation was restricted to rotation and linear (proportional) scaling to achieve overlap of the images from the two modalities.

Live-cell imaging and kymograph analysis. Undifferentiated murine podocytes were transiently transfected using Amaxa nucleofection (Lonza, Allendale, NJ) with plasmids encoding constitutively active Rac1 or RhoA. Transfected podocytes were cultured on collagen I-coated glass-bottom dishes overnight and were serum starved for 6 h to arrest baseline membrane ruffling. Rac1-transfected podocytes were imaged in the serum-starved state, while 10% FBS was added to Rho-transfected podocytes 10 min prior to imaging in order to induce membrane ruffling. Sequential images were obtained with an Olympus FluoView FV1000 microscope every 10 s for a 20-min duration, and movies were assembled using Olympus FluoView software. The ImageJ plug-in Multiple Kymograph (http://rsbweb.nih.gov/ij) was used to generate kymographs at 5 different locations of maximum membrane ruffling for each cell imaged (27). Ten actin spikes were measured for each kymograph, and the average length (ruffling index) was determined as described previously (28).

Rac1 pulldown assay. The glutathione *S*-transferase (GST)-tagged p21 binding domain of PAK1 (PBD) was expressed in *Escherichia coli* BL21(DE3) and was purified using glutathione-agarose beads. For the active Rac1 pulldown assay, whole-kidney lysates were generated by homogenizing the kidneys in cell lysis buffer (50 mM Tris-HCl [pH 7.5], 150 mM NaCl, 5 mM $MgCl_2$, 10% glycerol, 1% NP-40, 1 mM dithiothreitol [DTT], 1 mM phenylmethylsulfonyl fluoride [PMSF], 10 μg aprotinin, 10 μg leupeptin; aprotinin, leupeptin, DTT, and PMSF were freshly added) and isolating the supernatant. Equal volumes of the lysates were incubated with GST-PBD beads. Rac1-GTP bound to the beads (active Rac1) was eluted with Laemmli sample buffer and was examined by immunoblotting.

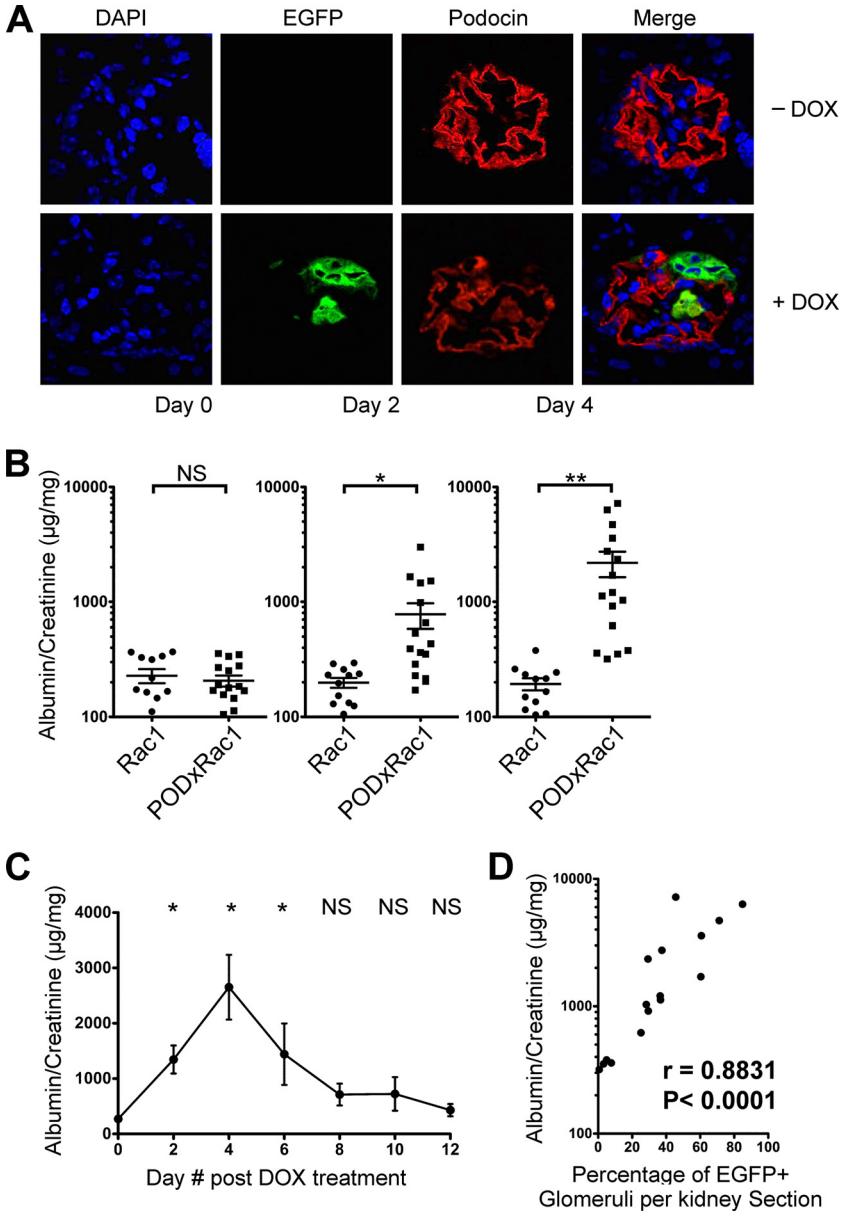

FIG 3 Podocyte-specific expression of CA-Rac1 causes proteinuria. (A) (Top) Without DOX induction, EGFP_CA-Rac1 is not expressed in POD×Rac1 mice. (Bottom) After a 4-day DOX induction, the EGFP_CA-Rac1 transgene (green) is specifically expressed in glomerular podocytes, as confirmed by immunofluorescence colocalization with the podocyte marker podocin (red). (B) DOX treatment induced a fast onset of proteinuria in POD×Rac1 mice. Urine samples were collected from single transgenic EGFP_CA-Rac1 mice and from DOX-induced double transgenic POD×Rac1 mice at the indicated time points. Proteinuria was quantitated by measuring the albumin/creatinine ratio for each sample. Each data point represents the albumin/creatinine ratio for a single mouse, measured at the indicated time point. NS, not significant. (C) DOX-induced proteinuria is transient in POD×Rac1 mice. (D) The frequency of $EGFP^+$ glomeruli correlated positively with the level of proteinuria (albumin/creatinine ratio) (Pearson's *r*, 0.8831; *P*, <0.0001).

Immunoblotting for protein in urine. Fifty microliters of trichloroacetic acid (TCA) was added to a 200-μl urine sample in order to precipitate protein. After a 10-min incubation, the precipitate was pelleted at 14,000 rpm for 10 min in a tabletop microcentrifuge. The supernatant was discarded, and the pellet was washed once with ice-cold acetone. The pellet was heated briefly to 95°C in order to evaporate residual acetone. After the addition of Laemmli sample buffer, the samples were resolved by SDS-PAGE, transferred to nitrocellulose membranes, and immunoblotted for WT1 and EGFP by using the antibodies described above.

RESULTS

Rho-family GTPases induce distinct effects on the actin cytoskeleton in cultured murine podocytes. To test the effects of Rho GTPase activation on the podocyte actin cytoskeleton *in vitro*, we first transfected an immortalized murine podocyte line with enhanced green fluorescent protein (EGFP) fused to constitutively active versions of Rac1 (EGFP_CA-Rac1) and RhoA (EGFP_CA-RhoA). Actin fibers and focal adhesions were visualized with phalloidin and vinculin, respectively. Constitutively active Rho (CA-

Rho) increased the number of stress fibers and focal adhesions in podocytes (Fig. 1A). In contrast, CA-Rac1 expression in podocytes induced membrane spreading and lamellipodium formation, resulting in large, round, flattened cells (Fig. 1A).

Since foot process effacement might reflect increased podocyte motility (29), we next asked if these changes in cell morphology correlated with changes in podocyte membrane dynamics. Using live-cell imaging, we quantitated membrane motility using kymograph analysis as described previously (19). Podocytes expressing CA-Rac1 showed increased membrane ruffling relative to that of wild-type cells after serum starvation (Fig. 1B; see also Videos S1 and S2 in the supplemental material). The addition of serum induced membrane ruffling in wild-type cells, which was largely suppressed in podocytes expressing CA-RhoA (Fig. 1C; see also Videos S3 and S4 in the supplemental material). These experiments confirmed that activation of Rac1 and activation of RhoA produce marked changes in the podocyte actin cytoskeleton and in membrane dynamics. Active Rac1 induced lamellipodium formation and increased membrane motility in podocytes, while active RhoA stabilized the cytoskeleton and suppressed membrane motility.

Generation of inducible EGFP_CA-Rac1 transgenic mice. Our *in vitro* results suggested that Rac1 activation might have significant effects on podocyte function *in vivo*. Recent studies showed that altered RhoA activity could play a pathogenic role in podocytes *in vivo* (8, 9). However, a direct pathogenic role for Rac1 activation in podocytes had not been tested *in vivo*. We therefore generated a transgenic mouse model that would allow for inducible expression of EGFP_CA-Rac1. Using homologous recombination, we targeted the EGFP_CA-Rac1 transgene to the *Hprt1* locus in ES cells (20, 21) (Fig. 2A). Cells with successful homologous recombination of the transgene into the *Hprt1* locus were selected on the basis of their growth in the presence of 6-thioguanine, which is toxic to cells harboring a functional *Hprt1* allele. Targeted gene insertion was confirmed by PCR (Fig. 2B and C), and recombinant ES cells were microinjected into blastocysts to generate chimeric mice.

EGFP_CA-Rac1 expression in podocytes causes rapid-onset but transient proteinuria. To induce podocyte-specific expression, we crossed the EGFP_CA-Rac1 transgenic mice with another transgenic line of mice with an rtTA transgene driven by the human podocin promoter, *NPHS2* (POD-rtTA mice) (22). In double transgenic (POD×Rac1) mice fed DOX, EGFP expression was detectable as early as 4 days after induction. To validate the functionality of the EGFP_CA-Rac1 transgene product, we used the p21 binding domain of PAK1 (PBD) to precipitate EGFP_CA-Rac1 from whole-kidney lysates of DOX-treated double transgenic mice (Fig. 2D). EGFP_CA-Rac1 protein was then immunoblotted using an anti-GFP antibody. EGFP_CA-Rac1 was readily detectable in kidney lysates from DOX-treated mice but was not detected in the absence of DOX. Expression of the transgene was barely detectable in the whole-kidney lysate, a finding consistent with the restriction of transgene expression to podocytes only. The expression of the CA-Rac1 transgene in podocytes was confirmed by colocalization with the podocyte-specific marker (podocin) by immunofluorescence microscopy (Fig. 3A). However, the CA-Rac1 transgene was expressed in only a portion of podocytes, and this level of expression was variable from one glomerulus to the next and from one mouse to another.

After 2 days of induction with DOX, POD×Rac1 mice developed significant proteinuria, while no proteinuria was detected in single transgenic control mice. Proteinuria reached its peak on day 4 and then began to abate around 1 week postinduction (Fig. 3B and C). DOX treatment for as long as 3 months did not result in progressive renal dysfunction or significant histologic alterations. Given the variable expression of the transgene, we assessed whether the level of proteinuria correlated with the level of expression (Fig. 3D). The magnitude of proteinuria correlated positively with the frequency of EGFP-positive glomeruli. The kinetics of proteinuria were similar for all POD×Rac1 mice: proteinuria began around day 2 and abated after day 7 (Fig. 3C). These experiments showed that podocyte-specific expression of CA-Rac1 induced rapid and transient proteinuria that correlated with the level of transgene expression.

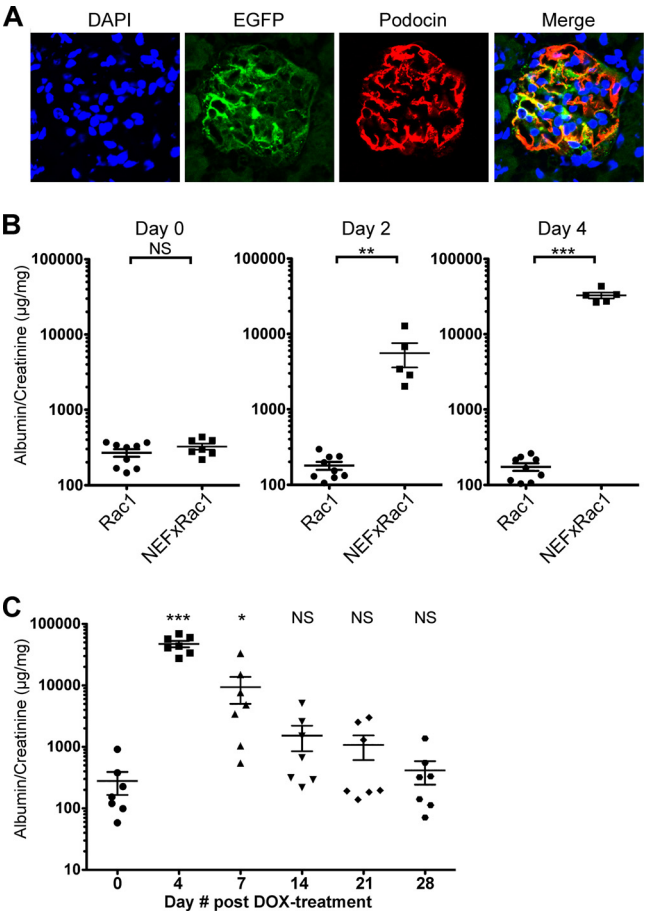

FIG 4 EGFP_CA-Rac1 expression driven by NEF-rtTA induces more robust transgene expression and transient proteinuria. (A) NEF-rtTA mice were generated and were crossed with EGFP_CA-Rac1 transgenic mice to generate NEF×Rac1 mice. After 4 days of DOX treatment, there was robust expression of the EGFP_CA-Rac1 transgene (green) in podocytes, which were labeled with the podocyte marker podocin (red). (B) Like POD×Rac1 mice, NEF×Rac1 mice were treated with DOX for various times, and proteinuria was measured in the urine samples collected. Compared to the single transgenic (EGFP_CA-Rac1 only) control mice, NEF×Rac1 mice exhibited significant proteinuria as early as 2 days after induction. Each data point represents the albumin/creatinine ratio from a single mouse measured at the indicated time point. (C) As with POD×Rac1 mice, the proteinuria in NEF×Rac1 mice peaked around day 4 and then returned to baseline in 28 days. Each data point represents the albumin/creatinine ratio from a single mouse measured at the indicated time point.

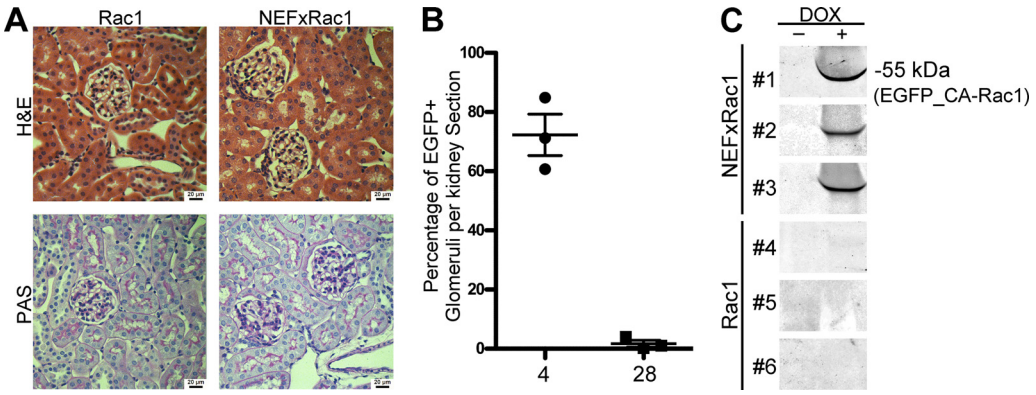

FIG 5 No obvious pathological changes were detected by histological analysis of DOX-induced NEF×Rac1 mice, and the transgene-positive podocytes were lost after prolonged DOX treatment. (A) Hematoxylin-and-eosin (H&E)- and periodic acid-Schiff (PAS)-stained kidney sections from NEF×Rac1 mice induced with DOX for 4 days. (Left) Control kidney samples; (right) NEF×Rac1 tissues. (B) Kidney samples were harvested from 3 NEF×Rac1 mice treated with DOX for 4 days or 28 days. For each kidney section, the percentage of EGFP-positive glomeruli was counted. (C) Immunoblotting of urinary protein for EGFP_CA-Rac1. Six mice were induced with DOX for 2 days, and urine samples were collected before DOX treatment (−DOX) and at day 2 post-DOX treatment (+DOX). Total protein was precipitated by TCA and was resolved with SDS sample buffer. We detected chimeric EGFP_CA-Rac1 protein in NEF×Rac1 urine samples (samples 1 to 3) after DOX induction but not before DOX induction. Rac1 single transgenic mice were used as negative controls.

NEF-rtTA-driven EGFP_CA-Rac1 expression in podocytes results in higher transgene expression and more-severe proteinuria. We considered that the patchy and uneven expression of CA-Rac1 might be due to silencing of the POD-rtTA transgene. To circumvent this problem, a new transgenic mouse line expressing a modified form of rtTA (rtTA-3G) under the control of the mouse nephrin (*Nphs1*) promoter was generated (NEF-rtTA) (34) and was bred to our EGFP_CA-Rac1 mice. Examination of kidneys from double transgenic (NEF×Rac1) mice after 4 days of DOX treatment showed a greater proportion of glomeruli and higher numbers of podocytes expressing the transgene than those for POD×Rac1 mice (Fig. 4A). However, ubiquitous expression of the transgene in podocytes still was not seen. This increased expression and distribution of the CA-Rac1 transgene did, however, correlate with a faster onset and higher levels of proteinuria than those for POD×Rac1 mice (Fig. 4B). The proteinuria in NEF×Rac1 mice persisted after 1 week of DOX treatment (Fig. 4C). However, as with POD×Rac1 mice, proteinuria peaked at day 4 and decreased gradually over time (Fig. 4C).

After mice were exposed to DOX for 28 days, we could not detect any EGFP_CA-Rac1-expressing podocytes in kidney sections from either POD×Rac1 or NEF×Rac1 mice (Fig. 5B). We hypothesized that this might be due to shedding of the transgene-expressing cells into the urine during the proteinuric phase. To investigate this possibility, we collected urine samples before and after DOX treatment and tested them for the presence of cells expressing EGFP_CA-Rac1 by immunoblotting with an anti-GFP antibody. In the absence of DOX treatment, EGFP_CA-Rac1 was not detected (Fig. 5C). After DOX treatment, EGFP_CA-Rac1 was readily detected in the urine samples of NEF×Rac1 mice. Cytospin preparations from the same mice showed occasional EGFP_CA-Rac1-expressing podocytes (data not shown).

EGFP_CA-Rac1 induces foot process effacement, but without other histological changes in the glomerulus. Next, the morphology of podocytes expressing CA-Rac1 was assessed by both light and electron microscopy. Glomeruli from DOX-induced Rac1 single transgenic mice and NEF×Rac1 mice were unremarkable by light microscopy (Fig. 5A). No obvious abnormalities were detected even after 1 month of continuous DOX induction. Transmission electron microscopy showed segmental effacement of podocyte foot processes in POD×Rac1 glomeruli (Fig. 6A), a finding consistent with uneven transgene expression. To test this, we used a superresolution fluorescence imaging method, *s*tochastic *o*ptical *r*econstruction *m*icroscopy (STORM). STORM achieves nanometer resolution by sequential imaging of a sparse subset of fluorescently labeled molecules (24). Sections of kidney tissues from NEF×Rac1 mice on day 4 after DOX induction were stained with fluorescently tagged antibodies for EGFP (to localize CA-Rac1) and laminin β2 (to detect the glomerular basement membrane) and were examined by STORM. After STORM imaging, the coverslip with attached tissue was lifted off the slide and was reprocessed for freeze-etch electron microscopy. EM-STORM correlations (Fig. 6B and C) showed that only the EGFP_CA-Rac1-expressing podocytes had effaced foot processes, while adjacent non-EGFP_CA-Rac1-expressing podocytes had intact foot processes (Fig. 6C). These studies are consistent with the hypothesis that the presence of the EGFP_CA-Rac1 transgene specifically induces foot process effacement in podocytes. They also provide an explanation for the segmental foot process effacement seen by TEM.

CA-Rac1 decreases podocin and nephrin levels via proteasomal degradation. During our examination of double transgenic kidneys by immunofluorescence microscopy (Fig. 3A and 4A), we noted that in both POD×Rac1 and NEF×Rac1 mice, EGFP_CA-Rac1 expression appeared to be inversely correlated with podocin and nephrin levels (Fig. 7A and C). Quantitative correlation of the pixel intensity of EGFP with those of podocin and nephrin showed significant negative correlations (Fig. 7B, D, E, and F). To test whether Rac1 activation might directly downregulate podocin protein levels, cultured podocytes were transiently transfected with an empty vector, EGFP_CA-Rac1, or EGFP_CA-RhoA, and podocin levels were analyzed by immunoblotting. In five independent experiments, CA-Rac1 diminished podocin levels by about 50% from those with the vector control, while CA-RhoA had no effect (Fig. 7G). We measured the levels of podocin mRNA in these podocytes by quantitative PCR and found no significant

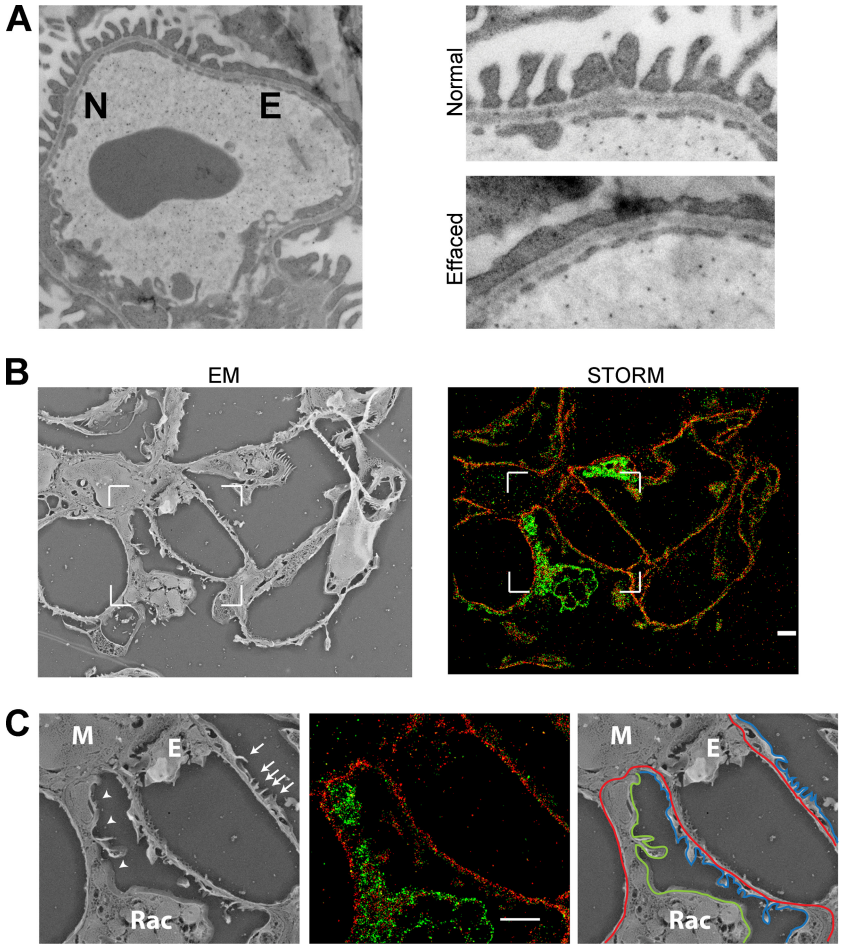

FIG 6 EGFP_CA-Rac1 expression in podocytes is associated with foot process effacement *in vivo*. (A) (Left) Examination of kidney tissues from DOX-treated POD×Rac1 mice by transmission electron microscopy demonstrates segmental effacement (E) of podocyte foot processes, while the foot processes of neighboring podocytes are intact and appear normal (N). (Right) The same areas at a higher magnification. (B) Scanning electron microscopy (left) and STORM (right) imaging techniques were performed on the same glomerulus from a NEF×Rac1 mouse treated with DOX for 4 days. For STORM imaging, the sample was stained for laminin β2 (red) and EGFP (green) in order to label EGFP_CA-Rac1-expressing podocytes. The boxed area is examined in detail in panel C. (C) Correlation of STORM and EM images demonstrates that EGFP-CA-Rac1-expressing podocytes have effaced foot processes, while neighboring non-transgene-expressing podocytes retain intact foot processes. (Left) Capillary loops with effaced foot processes (arrowheads) and intact foot processes (arrows). (Center) STORM imaging of the same area with laminin β2 (red) and EGFP (green). (Right) Schematized representation of the STORM data overlaid on the EM image. The glomerular basement membrane marked by laminin β2 is outlined in red. The EGFP_CA-Rac1 podocyte with its effaced foot processes is outlined in green. The intact foot processes of non-transgene-expressing podocytes are outlined in blue. M, mesangial cell; E, endothelial cell.

difference, suggesting that the decrease in podocin expression was not mediated by transcriptional downregulation (Fig. 7H). The decrease in podocin levels could be blocked by the proteasome inhibitor MG132, suggesting that Rac1 activation induces podocin degradation *in vitro*, at least in part via the proteasomal pathway (Fig. 7I).

DISCUSSION

The glomerular podocyte, with its arbor of interdigitating foot processes, is the critical final component of the kidney's filtration barrier. The elaborate actin-based cytoskeleton of the podocyte's foot process is effaced in proteinuric kidney diseases. Since actin reorganization mediated by Rho-family GTPases is a well-established mechanism for cell shape change, we and others have attempted to ask directly how specific Rho GTPase activation regulates podocyte morphology *in vivo*.

Previous studies used an approach similar to ours to study the role of RhoA in podocytes by generating constitutively active and dominant negative (DN) inducible RhoA transgenic mouse lines (8, 9). Both approaches resulted in podocyte dysfunction, albeit with different kinetics. In both models, proteinuria developed relatively slowly, over several weeks to months. Given the rapidity with which Rho-family GTPases can induce actin cytoskeletal changes *in vitro*, those findings raise the possibility that proteinuria in those systems is due to indirect effects of transgene expression in podocytes rather than to a direct signaling effect of RhoA. In addition, the mechanism of foot process effacement directed by RhoA activation was not directly addressed in those studies.

In our transgenic mouse model, expression of constitutively active Rac1 (CA-Rac1) produced a rapid onset (~48 h) of proteinuria that correlated with the degree of transgene expression. While the NEF-rtTA transgene was expressed in a larger percentage of podocytes than the POD-rtTA transgene, neither system resulted in transgene expression in all podocytes. Uneven expres-

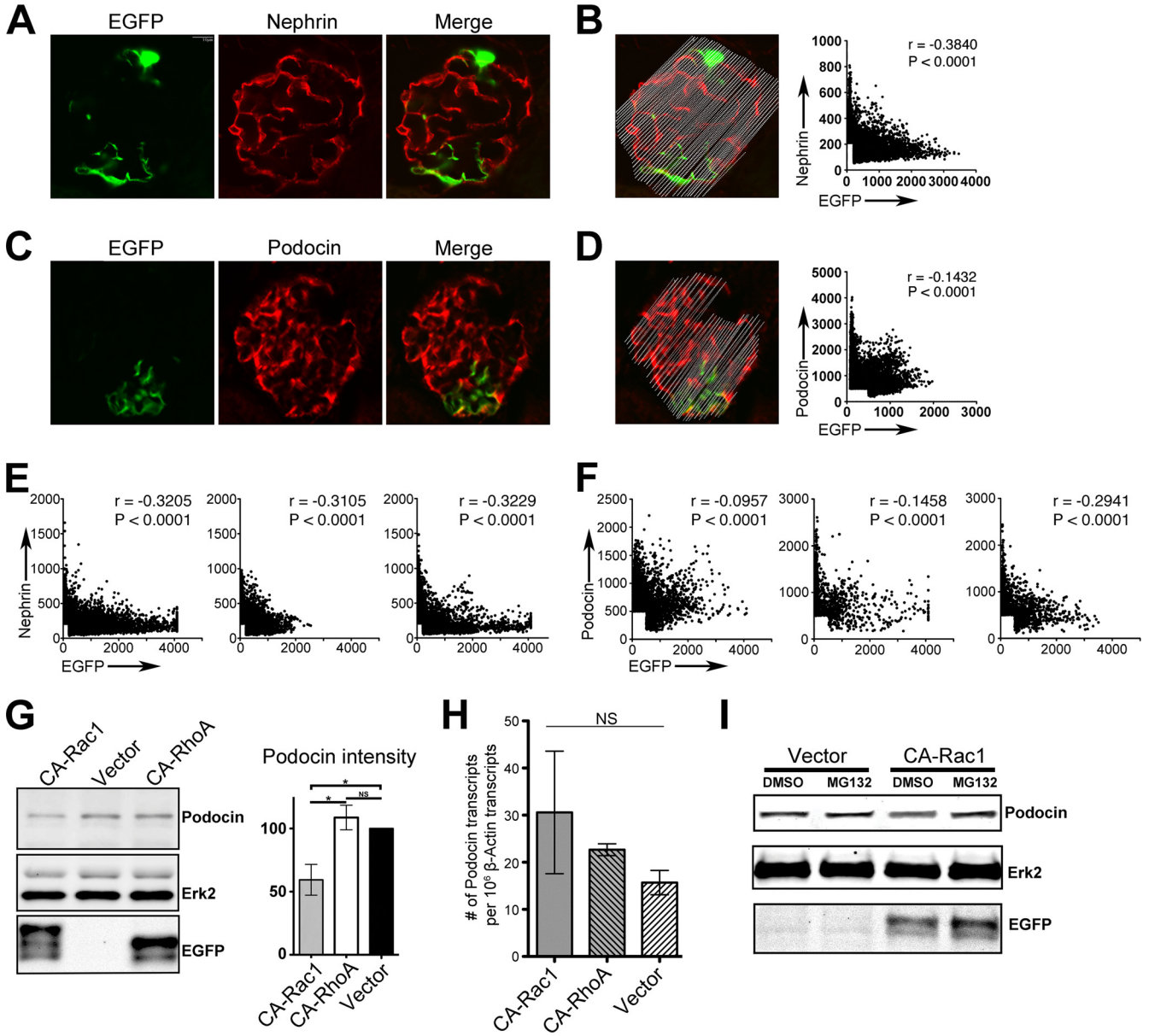

FIG 7 EGFP_CA-Rac1 expression correlates with reduced expression of podocin and nephrin. (A through D) A NEF×Rac1 mouse was induced with DOX for 4 days, and glomeruli were stained for nephrin (A) and podocin (C), both shown in red. There is decreased expression of nephrin and podocin in podocytes expressing the EGFP_CA-Rac1 transgene. Quantitation of pixel intensity across the glomerulus demonstrates the separation of nephrin (Pearson's r, −0.3840; P, <0.0001) (B) and podocin (Pearson's r, −0.1432; P, <0.0001) (D) signals from EGFP_CA-Rac1 signals. (E and F) Additional measurements of nephrin (E) and podocin (F) in three other glomeruli. (G) Expression of EGFP_CA-Rac1 but not of EGFP_CA-RhoA in cultured podocytes reduces podocin protein levels. (Left) Cultured podocytes were electroporated with an EGFP_CA-Rac1 or EGFP_CA-RhoA expression plasmid. Protein lysates were immunoblotted for podocin, Erk2, and EGFP. EGFP_CA-Rac1 reduced podocin protein levels from those with the empty-vector control and EGFP_CA-RhoA. (Right) Densitometric quantitation of podocin levels normalized to Erk2 levels in three independent experiments. An asterisk indicates a significant difference ($P < 0.05$) by the unpaired t test. NS, not significant. (H) Quantitative PCR for podocin and β-actin was performed with cDNA preparations of podocytes expressing CA-Rac1, CA-RhoA, or a vector control. (I) The reduction in podocin levels can be rescued by treatment with the proteasomal inhibitor MG132 but not with the vehicle (dimethyl sulfoxide [DMSO]) alone.

sion of the EGFP_CA-Rac1 transgene could explain the segmental foot process effacement detected by electron microscopy. Using STORM imaging and freeze-etch electron microscopy correlation techniques that we developed recently (25), we confirmed that effaced foot processes correlated with GFP-positive cells. In contrast to the slow onset of proteinuria with RhoA transgenic mice, the rapid onset and dose-responsive nature of proteinuria induced by CA-Rac1 expression provides strong evidence for a direct signaling role for Rac1 activation in causing foot process effacement and proteinuria.

While the onset of proteinuria in CA-Rac1-expressing mice was rapid, the proteinuria induced was only transient. This correlated with a permanent loss of EGFP_CA-Rac1 transgene expression in the kidney sections. Since GFP could not be detected in the

kidneys of mice receiving long-term DOX treatment, we suspected that chronic Rac1 activation resulted in the shedding of podocytes into the urine. This is not surprising, because Rac activation inhibits Rho activity, and Rho activation is involved in cell adhesion. Immunoblotting showed the presence of transgene-derived protein in urine samples from DOX-induced NEF×Rac1 mice (Fig. 4C). Assays of cell death due to apoptosis (terminal deoxynucleotidyltransferase-mediated dUTP-biotin nick end labeling [TUNEL]) were negative.

The efficiency of CA-Rac1 transgene expression differed for the two different rtTA driver lines and even for mice with the same rtTA driver line. This difference necessitated the direct correlation of transgene expression in kidney sections with the degree of proteinuria. The reason for this variability in expression is unclear, but it needs to be accounted for when one is using both of these transgenic lines. It is well known that epigenetic silencing can suppress transgene expression over time (30). It is also possible that the incomplete expression of our CA-Rac1 transgene is related to other epigenetic factors that affect the expression of both the rtTA and EGFP_CA-Rac1 transgenes.

We did not observe any progressive renal dysfunction or focal and segmental glomerulosclerosis (FSGS) in CA-Rac1-expressing mice after prolonged DOX treatment, in contrast to observations for CA-RhoA transgenic mice (9). This may be attributed to the low frequency of EGFP_CA-Rac1-expressing podocytes in our systems, since in a rat model of tunable podocyte loss, approximately 20 to 40% podocyte depletion was required before FSGS was consistently observed (31).

The presence of EGFP_CA-Rac1 reduced podocin protein expression both *in vivo* and in cultured podocytes. This reduction was mediated, at least in part, by proteasomal degradation, as evidenced by the fact that it could be blocked *in vitro* with proteasome inhibitors. Because we could not detect CA-Rac1-positive cells after extended DOX treatment, we suspect that the transgene-expressing podocytes were lost and that compensatory mechanisms were deployed to maintain podocyte function (32, 33). These compensatory mechanisms might explain the resolution of proteinuria over time in CA-Rac1-expressing mice. Our studies suggest that the development of tools to detect the activation of endogenous Rac1 and RhoA in podocytes might be clinically useful and that the decreased expression of nephrin and podocin could potentially be used as a surrogate marker for Rac activation.

ACKNOWLEDGMENTS

We are grateful for the help of Jacqueline Mudd from the Murine Embryonic Stem Cell Core of the Siteman Cancer Center in generating the recombinant embryonic stem cells. We thank Michael White from the Transgenic Knockout Microinjection Core of the Department of Pathology and Immunology for technical assistance in generating the chimeric mice and Jaclynn Lett for EM sample preparation and assistance with imaging (Microscopy and Digital Imaging Core in the Research Center for Auditory and Visual Studies, Department of Otolaryngology, Washington University School of Medicine; funded by NIH grant P30DC004665). We appreciate Rudolf Jaenisch for sharing the KH2 ES cell line and Takako Sasaki for providing the laminin β2 antiserum. We also thank Jiancheng Hu for reagents and helpful discussions.

This research was supported by the Howard Hughes Medical Institute and NIH grant R01DK058366 to A. S. Shaw and by NIH grant R21DK095419 to J. H. Miner.

We declare no conflict of interest.

REFERENCES

1. **Greka A, Mundel P.** 2012. Cell biology and pathology of podocytes. Annu. Rev. Physiol. **74:**299–323.
2. **Blattner SM, Hodgin JB, Nishio M, Wylie SA, Saha J, Soofi AA, Vining C, Randolph A, Herbach N, Wanke R, Atkins KB, Gyung Kang H, Henger A, Brakebusch C, Holzman LB, Kretzler M.** 15 May 2013. Divergent functions of the Rho GTPases Rac1 and Cdc42 in podocyte injury. Kidney Int. [Epub ahead of print.] doi:10.1038/ki.2013.175.
3. **Hall A.** 1998. Rho GTPases and the actin cytoskeleton. Science **279:**509–514.
4. **Faul C, Asanuma K, Yanagida-Asanuma E, Kim K, Mundel P.** 2007. Actin up: regulation of podocyte structure and function by components of the actin cytoskeleton. Trends Cell Biol. **17:**428–437.
5. **Scott RP, Hawley SP, Ruston J, Du J, Brakebusch C, Jones N, Pawson T.** 2012. Podocyte-specific loss of Cdc42 leads to congenital nephropathy. J. Am. Soc. Nephrol. **23:**1149–1154.
6. **Burridge K, Doughman R.** 2006. Front and back by Rho and Rac. Nat. Cell Biol. **8:**781–782.
7. **Wildenberg GA, Dohn MR, Carnahan RH, Davis MA, Lobdell NA, Settleman J, Reynolds AB.** 2006. p120-catenin and p190RhoGAP regulate cell-cell adhesion by coordinating antagonism between Rac and Rho. Cell **127:**1027–1039.
8. **Zhu L, Jiang R, Aoudjit L, Jones N, Takano T.** 2011. Activation of RhoA in podocytes induces focal segmental glomerulosclerosis. J. Am. Soc. Nephrol. **22:**1621–1630.
9. **Wang L, Ellis MJ, Gomez JA, Eisner W, Fennell W, Howell DN, Ruiz P, Fields TA, Spurney RF.** 2012. Mechanisms of the proteinuria induced by Rho GTPases. Kidney Int. **81:**1075–1085.
10. **Pertz O, Hodgson L, Klemke RL, Hahn KM.** 2006. Spatiotemporal dynamics of RhoA activity in migrating cells. Nature **440:**1069–1072.
11. **Kraynov VS, Chamberlain C, Bokoch GM, Schwartz MA, Slabaugh S, Hahn KM.** 2000. Localized Rac activation dynamics visualized in living cells. Science **290:**333–337.
12. **Asanuma K, Yanagida-Asanuma E, Faul C, Tomino Y, Kim K, Mundel P.** 2006. Synaptopodin orchestrates actin organization and cell motility via regulation of RhoA signalling. Nat. Cell Biol. **8:**485–491.
13. **Yanagida-Asanuma E, Asanuma K, Kim K, Donnelly M, Young Choi H, Hyung Chang J, Suetsugu S, Tomino Y, Takenawa T, Faul C, Mundel P.** 2007. Synaptopodin protects against proteinuria by disrupting Cdc42:IRSp53:Mena signaling complexes in kidney podocytes. Am. J. Pathol. **171:**415–427.
14. **Asanuma K, Kim K, Oh J, Giardino L, Chabanis S, Faul C, Reiser J, Mundel P.** 2005. Synaptopodin regulates the actin-bundling activity of α-actinin in an isoform-specific manner. J. Clin. Invest. **115:**1188–1198.
15. **Huber TB, Kwoh C, Wu H, Asanuma K, Godel M, Hartleben B, Blumer KJ, Miner JH, Mundel P, Shaw AS.** 2006. Bigenic mouse models of focal segmental glomerulosclerosis involving pairwise interaction of CD2AP, Fyn, and synaptopodin. J. Clin. Invest. **116:**1337–1345.
16. **Shibata S, Nagase M, Yoshida S, Kawarazaki W, Kurihara H, Tanaka H, Miyoshi J, Takai Y, Fujita T.** 2008. Modification of mineralocorticoid receptor function by Rac1 GTPase: implication in proteinuric kidney disease. Nat. Med. **14:**1370–1376.
17. **Gee HY, Saisawat P, Ashraf S, Hurd TW, Vega-Warner V, Fang H, Beck BB, Gribouval O, Zhou W, Diaz KA, Natarajan S, Wiggins RC, Lovric S, Chernin G, Schoeb DS, Ovunc B, Frishberg Y, Soliman NA, Fathy HM, Goebel H, Hoefele J, Weber LT, Innis JW, Faul C, Han Z, Washburn J, Antignac C, Levy S, Otto EA, Hildebrandt F.** 2013. ARHGDIA mutations cause nephrotic syndrome via defective RHO GTPase signaling. J. Clin. Invest. **123:**3243–3253.
18. **Gupta IR, Baldwin C, Auguste D, Ha KC, El Andalousi J, Fahiminiya S, Bitzan M, Bernard C, Akbari MR, Narod SA, Rosenblatt DS, Majewski J, Takano T.** 2013. ARHGDIA: a novel gene implicated in nephrotic syndrome. J. Med. Genet. **50:**330–338.
19. **Akilesh S, Suleiman H, Yu H, Stander MC, Lavin P, Gbadegesin R, Antignac C, Pollak M, Kopp JB, Winn MP, Shaw AS.** 2011. Arhgap24 inactivates Rac1 in mouse podocytes, and a mutant form is associated with familial focal segmental glomerulosclerosis. J. Clin. Invest. **121:**4127–4137.
20. **Doetschman T, Gregg RG, Maeda N, Hooper ML, Melton DW, Thompson S, Smithies O.** 1987. Targetted correction of a mutant HPRT gene in mouse embryonic stem cells. Nature **330:**576–578.
21. **Hooper M, Hardy K, Handyside A, Hunter S, Monk M.** 1987. HPRT-

deficient (Lesch-Nyhan) mouse embryos derived from germline colonization by cultured cells. Nature **326:**292–295.
22. **Shigehara T, Zaragoza C, Kitiyakara C, Takahashi H, Lu H, Moeller M, Holzman LB, Kopp JB.** 2003. Inducible podocyte-specific gene expression in transgenic mice. J. Am. Soc. Nephrol. **14:**1998–2003.
23. **Sasaki T, Mann K, Miner JH, Miosge N, Timpl R.** 2002. Domain IV of mouse laminin β1 and β2 chains: structure, glycosaminoglycan modification and immunochemical analysis of tissue contents. Eur. J. Biochem. **269:**431–442.
24. **Bates M, Huang B, Dempsey GT, Zhuang X.** 2007. Multicolor super-resolution imaging with photo-switchable fluorescent probes. Science **317:**1749–1753.
25. **Suleiman H, Zhang L, Roth R, Heuser JE, Miner JH, Shaw AS, Dani A.** 2013. Nanoscale protein architecture of the kidney glomerular basement membrane. eLife, **2:**e01149. doi:10.7554/eLife.01149.
26. **Dani A, Huang B, Bergan J, Dulac C, Zhuang X.** 2010. Superresolution imaging of chemical synapses in the brain. Neuron **68:**843–856.
27. **Abramoff MD, Magelhaes PJ, Ram SJ.** 2004. Image processing with ImageJ. Biophotonics Int. **11:**36–42.
28. **Moeller MJ, Soofi A, Braun GS, Li X, Watzl C, Kriz W, Holzman LB.** 2004. Protocadherin FAT1 binds Ena/VASP proteins and is necessary for actin dynamics and cell polarization. EMBO J. **23:**3769–3779.
29. **Mundel P, Reiser J.** 2010. Proteinuria: an enzymatic disease of the podocyte? Kidney Int. **77:**571–580.
30. **Whitelaw E, Sutherland H, Kearns M, Morgan H, Weaving L, Garrick D.** 2001. Epigenetic effects on transgene expression. Methods Mol. Biol. **158:**351–368.
31. **Wharram BL, Goyal M, Wiggins JE, Sanden SK, Hussain S, Filipiak WE, Saunders TL, Dysko RC, Kohno K, Holzman LB, Wiggins RC.** 2005. Podocyte depletion causes glomerulosclerosis: diphtheria toxin-induced podocyte depletion in rats expressing human diphtheria toxin receptor transgene. J. Am. Soc. Nephrol. **16:**2941–2952.
32. **Poulsom R, Little MH.** 2009. Parietal epithelial cells regenerate podocytes. J. Am. Soc. Nephrol. **20:**231–233.
33. **Appel D, Kershaw DB, Smeets B, Yuan G, Fuss A, Frye B, Elger M, Kriz W, Floege J, Moeller MJ.** 2009. Recruitment of podocytes from glomerular parietal epithelial cells. J. Am. Soc. Nephrol. **20:**333–343.
34. **Lin X, Suh JH, Go J, Miner JH.** Feasibility of repairing glomerular basement membrane defects in Alport syndrome. J. Am. Soc. Nephrol., in press.